Three-dimensional ghost imaging based on periodic diffraction correlation imaging

Yongchao Zhu (朱泳超), Jianhong Shi (石剑虹)*, Hu Li (李 虎), and Guihua Zeng (曾贵华)

State Key Laboratory of Advanced Optical Communication Systems and Networks,
Keyoratory Lab on Navigation and Location-based Service,
Department of Electronic Engineering, Shanghai Jiao Tong University,
Shanghai 200240, China
**Corresponding author: purewater@sjtu.edu.cn*

Received November 22, 2013; accepted April 23, 2014; posted online June 25, 2014

We experimentally demonstrate a three-dimensional (3D) ghost imaging method based on period diffraction correlation imaging. Compared with conventional ghost imaging, our method can easily retrieve the images of different focal planes. Due to the correlation between the disturbed object beam and the reference beams which do not pass through any scattering, the clear images can be periodically obtained in the uncovered zones even through a scattering medium. The analysis of the 3D imaging resolution reveals that the proper resolution for actual demand can be achieved by designing our devices. The implementation of this experiment is quite simple and low-cost. It facilitates the practical applications of ghost imaging.

OCIS codes: 110.1650, 110.6880, 110.0113.
doi: 10.3788/COL201412.071101.

As an intriguing method, ghost imaging (GI) has received great attention and achieved considerable development since it was experimentally demonstrated in 1995[1−11]. With its non-local feature and imaging superiority in optically harsh or noisy environments[12−15], GI is providing a novel and powerful imaging tool. In recent years, the focus of GI is increasingly shifting from the fundamental research to its practical application. Acquiring the three-dimensional (3D) information of objects is of great importance in a variety of fields.

The retrieval of "ghost" image is achieved by using two spatially correlated beams. The reference beam, which never interacts with the object, is measured with a multipixel detector (e.g., a charge-coupled device (CCD) camera). The object beam is collected with a bucket detector after illuminating the object. In conventional pseudo-thermal GI, a beam splitter (BS) is an indispensable optical component used for creating point-to-point correlation. Thus the optical calibration between the two beams and the synchronous control of the detectors make the 3D GI difficult. In 2008, an interesting GI mechanism without a BS named computational GI was proposed, in which a spatial light modulator (SLM) was applied[7]. Compressive GI was subsequently proposed to significantly reduce the required acquisition times and boost the recovered image quality[8,9]. Recently, Sun *et al*. published a paper in Science that detailed how they managed to use an altered style of computational GI to create accurate 3D images[16]. In 2012, to simplify the traditional GI system, we proposed the periodic diffraction correlation imaging (PDCI)[17]. Periodic speckle patterns are generated at the diffraction plane when light passes through a periodic pinhole array. One of the periodic speckle patterns is used as the object beam to illuminate the object, and the other correlated parts are the reference beams to be collected directly. With the correlation algorithm, multiple images can be periodically retrieved. Then the experimental realization of reflection-type PDCI was achieved by us[18], while our previous work focused only on the imaging of two-dimensional (2D) objects. Since the object and reference beams are in the same plane, the optical calibration and the synchronous control are not necessary any more. It makes the acquisition of the 3D information simple. By selecting the different focal planes which contain the structures of interest, the sectional images of a 3D object can be retrieved for 3D reconstruction.

Imaging through scattering or turbid medium is another interesting but challenging area. Over the past decades, there have been many attempts to reconstruct the interesting image of the object behind a scattering or turbid medium. One prominent way is to form an image using the fraction of the light ("ballistic" light) that is not scattered[19−22]. Such methods usually require the expensive devices or complex operations. In general, the weak ballistic light signal through a turbid medium is collected by detection systems utilizing time gating techniques. In a different field, there have recently been many activities in exploiting scattered light for imaging purposes, including the techniques of phase conjugation[23], spatial and temporal wavefront shaping[24,25], and turbid lens imaging[26]. Normally, the optical setup and implementation of these methods are not simple. For example, the wavefront shaping generates a focused spot behind the scattering medium, with a SLM or a time-reversal mirror. Consequently, raster scanning is required in this method. GI is a great technique for ignoring the scattering of the light through a turbid medium by generating correlated beams.

In this letter, we investigate the potential applications of PDCI in 3D imaging, and research its imaging ability through scattering mediums. We demonstrate a simple and low-cost confirmatory experiment of 3D GI based on PDCI. The images of two planar objects can be easily

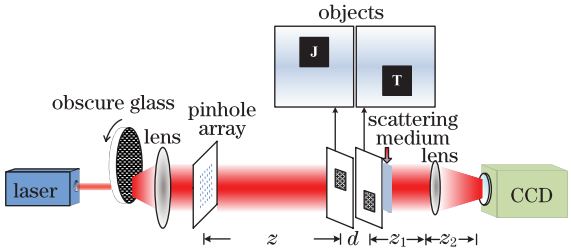

Fig. 1. (Color online) Schematic diagram of the experimental setup.

retrieved even through scattering medium. Through our analysis of the 3D resolution in our method, we also show that the proper resolution can be achieved by designing our devices.

The experimental schematic of our proposed approach is shown in Fig. 1. The light beam generated by a 633 nm He-Ne laser passed through an obscure glass. The obscure glass was driven by a stepper motor to rotate with a frequency of 0.9°/ms. A periodic pinhole array containing $M \times M = 50 \times 50$ pinholes was located after the obscure glass. The center-to-center distance a between adjacent pinholes is 100 μm. Then periodical speckle fields will be generated when the beam illuminates the pinhole array, and the period can be calculated by[17]

$$T = \frac{\lambda z}{a}, \tag{1}$$

where z is the diffraction distance.

To simulate the different planes of a real 3D object, two transmissive objects ("J" and "T", chromium layers with transparent characters deposited on the front surface of a lithography mask of 2 mm thickness) were placed at the axial distance z=375 mm. The distance d between the two plates is 20 mm. The two objects were illuminated by the bi-dimensionally periodical speckle fields. The respective periods of the speckle fields were T_1=2.37 mm and T_2=2.50 mm. The sizes of the objects should be smaller than the periods. Otherwise, the object information retrieved in the neighbor zones will be distorted. The sizes of the chromium layers are 5×5 (mm) and the widths of the characters are 1 mm. A 0.8-mm-thick scattering medium (a polyvinyl chloride sheet containing titanium dioxide particles) was placed after the lithography masks to hide the objects. Referring to general material injection molding parameters, the average size of the titanium dioxide particles is 0.35 μm. Then the scattering mean free paths is calculated to be $ls = 1/\rho\sigma_s \approx 71.2$ μm, where $\rho = 14.6 \times 10^{16}$ m^{-3} is the number density and $\sigma_s = 9.62 \times 10^{-14}$ m^2 is the scattering cross section. Therefore, the scattering medium is about 11.2 scattering mean free paths. The medium has the same width as the chromium layers, so the light passes through the characters will be scattered while the reference light can still be clearly recorded.

We used a lens of focal distance f =50 mm and a CCD as the detection system. The CCD contains 1024×512 pixels, and the pixel size equals 11×11 (μm). To satisfy the Gaussian lens imaging formula, the object distance z_1=100 mm and the image distance z_2=100 mm. Thus the image captured by the CCD just has the same size as the real object.

At first, we used the detection system to capture the images of object plane 1 ("J"). For the ith iteration, the speckle field varied with the rotary obscure glass. Light intensity distribution of the speckle field collected by the CCD was recorded as I_i, and the total light intensity of the light that penetrated the transparent characters was recorded as S_i. Then the image of the object 1 can be retrieved by

$$\mathrm{GI} = \langle \Delta I \Delta S \rangle = \langle (I - \langle I \rangle)(S - \langle S \rangle) \rangle, \tag{2}$$

where $N = 20000$ in our experiment is the total iterations and $\langle \cdot \rangle = \frac{1}{N} \sum_i (\cdot)$. For the imaging of object 2 ("T"), we just moved the whole detection system (including the lens and the CCD) backward d=20 mm while keeping the z_1 and z_2 unchanged. Then the focal plane of object 2 was captured by the CCD. We repeated the process N times as before. Here we experimentally demonstrate a prototype of 3D imaging through scattering medium. For a real 3D object, the detection system should move Δz each time to acquire the different focal planes. The smaller the Δz is, the more precise the 3D reconstruction will be. However, the minimum of Δz depends on the axial resolution δz, which will be further discussed.

Imaging results of the two objects through scattering medium can be retrieved respectively as shown in Fig. 2. As a result of the scattering medium, the light that penetrated the characters will be distorted. So we can hardly recognize the characters. The interesting object areas (the red block) in Figs. 2(a) and (b) were blurry in both experiments. While in Figs. 2(c) and (d), we can recover the object information (the blue block) in the uncovered neighborhood with high quality. The width of the characters in the images were both 98 pixels, in other words, 1.078 mm. The period of object 1 was 220 pixel (2.420 mm) and object 2 was 235 pixel (2.585 mm). The data accord well with the previous theoretical value.

In order to observe clearly, the object areas and the recovery areas were depicted in Fig. 3 for contrast. Figures 3(a) and (d) were captured directly by the CCD, and the sum of the 20000 photos were displayed in Figs. 3(b) and (e). It is more clear that the light was scattered as cloud cluster, in which situation the traditional imaging methods are incapable of recovering the objects. However, in Figs. 3(c) and (f), the two characters were well retrieved. The fundamental mechanism of GI is the spatially point-to-point correlation of either quantum entangled bi-photons or

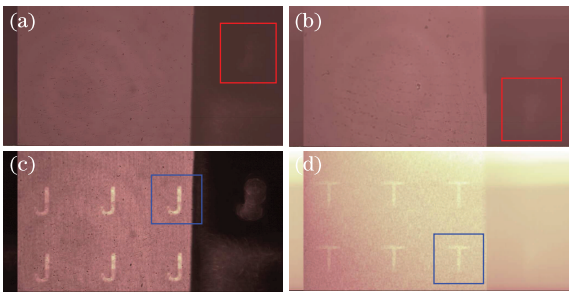

Fig. 2. (Color online) Imaging results through scattering medium. (a) Sum of 20000 photos of "J" and (b) sum of 20000 photos of "T". The object zones were blurry and the characters were hardly identifiable; The object images of (c) "J" and (d) "T" in the neighbor zones with PDCI.

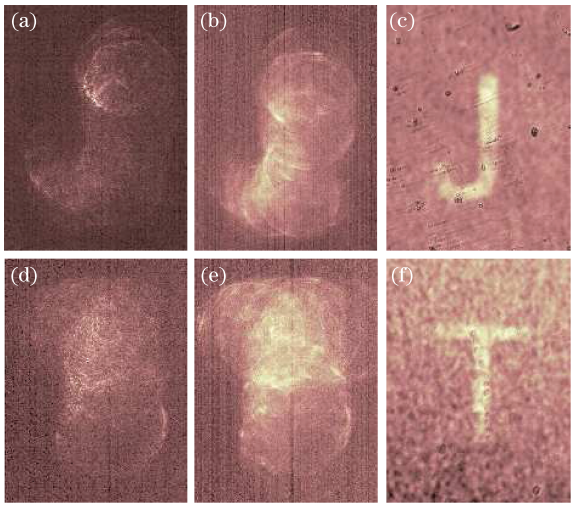

Fig. 3. (Color online) Detailed information in the region of interest (ROI). Object "J": (a) Captured directly by the CCD; (b) Sum of 20000 photos; (c) Image retrieved by PDCI; Object "T": (d) Captured directly by the CCD; (e) Sum of 20000 photos; (f) Image retrieved by PDCI.

thermal light. When the information of the object beam is distorted by a scattering medium, if we can collect the whole light intensity (or a portion of it), we can still retrieve the high quality image by correlating with the reference beam.

By theoretical analysis, the transverse resolution of PDCI is[17]

$$\delta x = \frac{T}{M} = \frac{\lambda z}{aM}, \tag{3}$$

where aM is the side length of the pinhole array. The transverse resolution depends on the parameters λ, z, and aM. In our experiment the transverse resolutions of "J" and "T" were 47.4 and 50 μm respectively. We can achieve higher transverse resolution by designing the parameters in Eq. (3). Choosing a laser of shorter wavelength λ, decreasing the distance z between the pinhole array and the object, or increasing the size aM of the pinhole array are all the effective approaches. For example, if we replace the pinhole array ($aM = 5$ mm) with a larger one ($aM = 10$ mm), the transverse resolution δx at the axial distance z=400 mm will improve from 71.5 to 38.5 μm. Decreasing the distance z from 400 to 200 mm while using the same pinhole array ($aM = 5$ mm) can achieve the similar result. If we do the both at the same time, δx will be improved approximately four times, as shown with the transverse coherence of the periodic speckle field in Fig. 4.

The axial resolution in the Fresnel zone can be calculated by[27,28]

$$\delta z \approx \frac{\delta x^2}{\lambda}. \tag{4}$$

The axial resolution along z-axis is usually much larger than the corresponding transverse resolution. However, Eq. (4) indicates that if we can achieve the δx as the wavelength, δz will also have the same magnitude as δx. With the more advanced devices (such as the higher-resolution CCD or the optical components of microscopic imaging), it is possible to achieve the proper 3D resolution for actual demand.

In conclusion, we give a further investigation of the previous PDCI method proposed by us, focusing on its potential applications in 3D GI. Inspired by the fact that the object beam and the reference beams are always in the same plane, we find it easier to realize the correlation imaging of different focal planes. The confirmatory experiment is achieved and demonstrated in detail. The analysis of the 3D resolution reveals that, our method can achieve proper 3D resolution for actual demand by designing our devices.

In addition, owing to the correlation of the reference beams which do not pass any scattering and the object

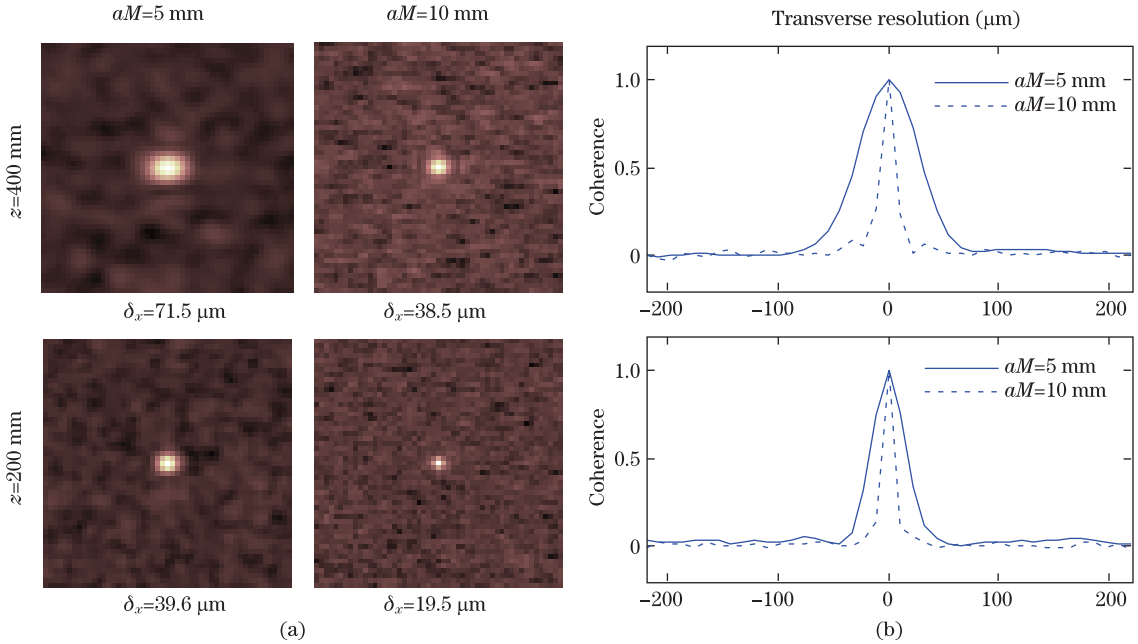

Fig. 4. (Color online) The improvement of transverse resolution with the increase of the size aM of the pinhole array, or with the decrease of the distance z. (a) The transverse coherence images of different periodic speckle fields; (b) the transverse resolution corresponding to the speckle fields under different parameters.

beam, our method can still retrieve the images when imaging the objects behind a scattering medium. Compared with conventional imaging mechanisms through scattering medium, the implementation of the proposed method is relatively simple and low-cost. Neither complex algorithms nor expensive devices (such as ultrashort pulsed laser, SLM, and so on) are required. The proposed imaging mechanism also has little restriction on the scattering medium as long as that a portion of the object light is able to pass through the scattering medium and be collected by the detection system.

Since it is of great importance in a variety of fields to acquire the 3D information of objects through scattering or turbid mediums (e.g., smoke, fog, or tissue), our work facilitates the practical applications of GI. The object axial position has to be known in advance, which makes it still unsuitable for far-field imaging. The acquisition times N seems large and the imaging process may be time-consuming, while they can be improved with high-speed detector and processing software. Since GI in general can only retrieve the shape or contour of the object, our method will inevitably not work for translucent objects that may vary the speckle pattern that propagates through it. For more practical application, the further work should focus on the reflection-type 3D imaging of a real object behind a scattering medium.

This work was supported by the National Natural Science Foundation of China under Grant Nos. 60970109 and 61170228.

References

1. T. B. Pittman, Y. H. Shih, D. V. Strekalov, and A. V. Sergienko, Phys. Rev. A. **52,** 3429 (1995).
2. R. S. Bennink, S. J. Bentley, and R. W. Boyd, Phys. Rev. Lett. **89,** 113601 (2002).
3. A. Gatti, E. Brambilla, M. Bache, and L. A. Lugiato, Phys. Rev. Lett. **93,** 093602 (2004).
4. F. Ferri, D. Magatti, A. Gatti, M. bache, E. Brambilla, and L. A. Lugiato, Phys. Rev. Lett. **94,** 183602 (2005).
5. A. Valencia, G. Scarcelli, M. D' Angelo, and Y. H. Shih, Phys. Rev. Lett. **94,** 063601 (2005).
6. Y. Bai and S. Han, Phys. Rev. A. **76,** 043828 (2007).
7. J. H. Shapiro, Phys. Rev. A. **78,** 061802 (2008).
8. O. Katz, Y. Bromberg, and Y. Silberberg, Appl. Phys. Lett. **95,** 131110 (2009).
9. Y. Bromberg, O. Katz, and Y. Silberberg, Phys. Rev. A. **79,** 053840 (2009).
10. D. Duan and Y. Xia, Chin. Opt. Lett. **10,** 031102 (2012).
11. Y. Zhang, J. Shi, H. Li, and G. Zeng, Chin. Opt. Lett. **12,** 011102 (2014).
12. W. Gong and S. Han, Opt. Lett. **36,** 394 (2011).
13. N. D. Hardy and J. H. Shapiro, Phys. Rev. A. **84,** 063824 (2011).
14. E. Meyers, K. S. Deacon, and Y. Shih, Appl. Phys. Lett. **98,** 111115 (2011).
15. M. Bina, D. Magatti, M. Molteni, A. Gatti, L. Lugiato, and F. Ferri, Phys. Rev. Lett. **110,** 083901 (2013).
16. B. Sun, M. P. Edgar, R. Bowman, L. E. Vittert, S. Welsh, A. Bowman, and M. J. Padgett, Science **340,** 844 (2013).
17. H. Li, Z. Chen, J. Xiong, and G. Zeng, Opt. Express. **20,** 2956 (2012).
18. H. Li, Y. Zhang, J. Shi, and G. Zeng, Appl. Phys. Lett. **102,** 201901 (2013).
19. M. R. Hee, J. A. Izatt, J. M. Jacobson, J. G. Fujimoto, and E. A. Swanson, Opt. Lett. **18,** 950 (1993).
20. S. C. W. Hyde, N. P. Barry, R. Jones, J. C. Dainty, and P. M. W. French, Opt. Lett. **20,** 1331 (1995).
21. D. D. Steele, B. L. Volodin, O. Savina, B. Kippelen, N. Peyghambarian, H. Röckel, and S. R. Marder, Opt. Lett. **23,** 153 (1998).
22. M. E. Zevallos, S. K. Gayen, M. Alrubaiee, and R. R. Alfanoa, Appl. Phys. Lett. **86,** 011115 (2005).
23. Z. Yaqoob, D. Psaltis, M. S. Feld, and C. Yang, Nat. Photonics **2,** 110 (2008).
24. O. Katz, E. Small, Y. Bromberg, and Y. Silberberg, Nat. Photonics **5,** 372 (2011).
25. A. P. Mosk, A. Lagendijk, G. Lerosey, and M. Fink, Nat. Photonics **6,** 283 (2012).
26. Y. Choi, T. D. Yang, C. Fang-Yen, P. Kang, K. J. Lee, R. R. Dasari, M. S. Feld, and W. Choi, Phys. Rev. Lett. **107,** 023902 (2011).
27. A. Gatti, D. Magatti, and F. Ferri, Phys. Rev. A. **78,** 063806 (2008).
28. A. Gatti, D. Magatti, and F. Ferri, Phys. Rev. A. **79,** 053831 (2009).